jove

A Murine Tail Lymphedema Model

Aladdin H. Hassanein[*,1], **Mithun Sinha**[*,1], **Colby R. Neumann**[1], **Ganesh Mohan**[1], **Imran Khan**[1], **Chandan K. Sen**[1]

[1] Department of Surgery, Indiana Center for Regenerative Medicine and Engineering, Indiana University School of Medicine

[*] These authors contributed equally

Corresponding Author

Aladdin H. Hassanein
ahassane@iu.edu

Citation

Hassanein, A.H., Sinha, M., Neumann, C.R., Mohan, G., Khan, I., Sen, C.K. A Murine Tail Lymphedema Model. *J. Vis. Exp.* (168), e61848, doi:10.3791/61848 (2021).

Date Published

February 10, 2021

DOI

10.3791/61848

URL

jove.com/video/61848

Abstract

Lymphedema is extremity swelling caused by lymphatic dysfunction. The affected limb enlarges because of accumulation of fluid, adipose, and fibrosis. There is no cure for this disease. A mouse tail model that uses a focal full thickness skin excision near the base of the tail, resulting in tail swelling, has been used to study lymphedema. However, this model may result in vascular comprise and consequent tail necrosis and early tail swelling resolution, limiting its clinical translatability. The chronic murine tail lymphedema model induces sustained lymphedema over 15 weeks and a reliable perfusion to the tail. Enhancements of the traditional murine tail lymphedema model include 1) precise full thickness excision and lymphatic clipping using a surgical microscope, 2) confirmation of post-operative arterial and venous perfusion using high resolution laser speckle, and 3) functional assessment using indocyanine green near infrared laser lymphangiography. We also use tissue nanotransfection technology (TNT) for novel non-viral, transcutaneous, focal delivery of genetic cargo to the mouse tail vasculature.

Introduction

Lymphedema is extremity swelling caused by lymphatic dysfunction. The affected limb enlarges because of the accumulation of fluid, adipose, and fibrosis[1]. Lymphedema affects 250 million people worldwide[2,3,4]. It is estimated that 20-40% of patients who undergo treatment for solid malignancies, such as breast cancer, melanoma, gynecological/urologic tumors, or sarcomas, develop lymphedema[2,4,5]. Morbidity from lymphedema includes recurrent infections, pain, and deformity[6]. There is no cure for this progressive, life-long disease. Current therapies are variaby effective[7] and include compression, complete decongestive therapy by physical therapists, excisional procedures, and microsurgical operations, including vascularized lymph node transfer and lymphovenous bypass[7,8,9,10,11,12,13,14]. The ideal treatment for lymphedema has yet to be discovered.

Studying the mechanism and therapy of lymphedema has been limited. There is an average delayed onset of one year following the lymphatic injury[15,16] and most individuals who experience iatrogenic insult with radiation and surgery do not develop lymphedema[4,6,17]. Although large animal

models, including canine, sheep, and pig have been described[18,19,20], the mouse tail model has been the most widely applied because of ease, cost, and reproducibilty. Mouse models for investigating lymphedema include a tail model, diptheria-toxin mediated lymphatic ablation, and axillary or popliteal lymph node dissection[21,22,23,24,25,26]. Most tail models use a focal, full thickness skin excision with lymphatic channel clipping that is performed near the base of the tail[22], resulting in tail swelling and histological features similar to human lymphedema[24,27,28,29]. However, the standard murine tail model typically spontaneous resolves in as few as 20 days and is accompanied by periodic tail necrosis[30]. The lymphedema mouse tail model extends a sustained lymphedema beyond 15 weeks, demonstrates confirmed arterial and venous patency, and allows functional lymphatic dysfunction assessment.

An murine tail model of lymphedema allows for evaluation of novel therapeutics to treat lymphedema. Gene-based strategies have been used in the mouse model mediated by viral vectors[31,32]. We also use a novel tissue nanotransfection technology (TNT) for genetic cargo delivery to the lymphedematous mouse tail. TNT facilitates direct, transcutaneous gene delivery using a chip with nanochannels in a rapid focused electric field[33,34,35,36]. The model includes using $TNT_{2.0}$ to allow for focal gene delivery of potential gene-based therapeutics to the lymphatic injury site of the mouse tail[35].

Protocol

The protocol follows the guidelines of the institution's animal research ethics committee. All animal experiments were approved by the Indiana University School of Medicine Institutional Animal Care and Use Committee. Animals were housed under a 12-hour light-dark cycle with food and water ad libitum.

1. Surgical Disruption of Mouse Tail Lymphatics

1. Use eight week-old C57BL/6 mice of equal gender distribution.
2. Place a mouse under general anesthesia in an induction chamber with 3-4% isoflurane in 100% oxygen followed by maintenance sedation at 1-3% during the procedure.
3. Administer 0.5 mg/kg sustained-release (SR) buprenorphine subcutaneously for pain control.
   NOTE: Additional analgesic drugs administered post-op: Carprofen once every 24 h for at least 48 h and Bupivacaine once either after the incision was made or before closing the incision, applied by dripping onto skin edges (lasts up to 4 – 6 h).
4. Position the mouse dorsally and prep the tail with 70% isopropyl alcohol.
5. Measure the tail diameter prior to the procedure at 5 mm increments starting 20 mm from the base of the tail using a caliper. These measurements will be used to calculate volume using the truncated cone equation[37].
6. Mark a 3 mm circumferential excision on the tail 20 mm from the base.
7. Perform a meticulous 3 mm full-thickness skin excision with a sterile surgical blade (size 15), leaving all the underlying vasculature intact under surgical microscopic magnification. Incise the superior circumferential mark (20 mm from tail base) first through the dermis followed by a circumferential full thickness incision 3 mm distlal to the first incision.

1. Make a perpendicular full thickness vertical incision to connect the two incisions. Use a toothed fine pickup to grasp a leading edge and use microscissors to carefully dissect deep within the avascular plane to the dermis and superficial to the vein adventitia.

8. Inject 0.1 mL of isosulfan blue (1%) subcutaneously proximal to tip of the tail.

9. Identify the two lymphatic channels adjacent to the lateral tail veins under the surgical microscope. The lymphatics will appear blue because of isosulfan injection. Transect the lymphatics using straight microsurgical scissors. Use the scissors to carefully dissect a plane between the lateral vein and the lymphatic. Then pass the tip of one scissor blade between the lymphatic vessel and the lateral vein and close the blades to transect the lymphatic vessel.

10. Dress the tail wound with a sterile adherent clear dressing. Check post-op incisions daily to ensure that they are not infected or bleeding and provide wound care for 2 weeks.

11. House the animals singly to prevent any further injury to the tail and to prevent the animals from biting each other, which would lead to surgical complications.

2. Tail vascular assessment with laser speckle contrast imaging

1. Anesthetize the mouse as in step 1.2.

2. To use laser speckle contrast imaging to visualize tail vascularity, set the width to 0.8 cm, height to 1.8 cm, point density to high, frame rate to 44 images/second, time to 30 seconds, and color photo to 1 per 10 seconds.

3. Evaluate the venous and arterial perfusion for patency. Qualitatively, continuity of flow should be visualized.

3. Functional lymphatic evaluation with near infrared laser angiography

1. Anesthetize the animal as in step 1.2

2. Reconstitute indocyanine green (ICG) (25 mg/10 mL) and administer 0.1 mL subcutaneously into the distal mouse tail near the tip.

3. Dim the room lights. Place near-infrared laser angiography in buffering setting followed by live capture.

4. Focal delivery of nucleic acid cargo to mouse tail using TNT

1. Anesthetize the animal as in step 1.2.

2. Exfoliate the mouse tail using topical skin exfoliation cream.

3. Immerse the mouse tail in collagenase solution (10 mg/mL) at 37 °C for 5 minutes.

4. Load DNA into the $TNT_{2.0}$ chip reservoir[35].

5. Place the $TNT_{2.0}$ silicone chip device over the desired focal site of delivery on the tail with nanoneedles in contact with the tail.

6. Place a positive electrical probe in the reservoir. Attach the negative probe to a 30 G needle and insert the needle subcutaneously into the tail to the site of delivery.

7. Apply square wave pulse electric stimulation (10 x 10 ms pulses, 250 V, 10 mA).

Representative Results

The technique for the mouse tail model for sustained lymphedema is shown in **Figure 1**. The figure exhibits the relevant anatomy of the mouse tail model. **Figure 2** demonstrates the progressive swelling and sustained persistant lymphedema in the mouse tail after lymphedema induction. The mouse tail volume, as calculated by the truncated cone equation, peaks at week 4 and plateaus to week 6 followed by gradual improvement that is sustained to week 15. Tail volume can be used as an outcome variable to assess the effect of therapeutic interventions for lymphedema in the model. In **Figure 3**, high resolution laser speckle for assessment of tail vasculature patency can be observed. This adds rigor to the model to ensure welling is secondary to lymphatic dysfunction rather than venous injury. The effect of interventions can then potentially translate to lymphedema treatment with greater confidence. **Figure 4** shows a functional lymphatic assessment performed via near infrared laser lymphangiography. This additional outcome variable allows for a functional lymphatic effect of interventions. **Figure 5** demonstrates the focal delivery of genetic cargo transcutaneously at the surgical site using tissue nanotransfection technology ($TNT_{2.0}$). $TNT_{2.0}$ facilitates point of care delivery of potential candidate gene-based therapeutics in this lymphedema model.

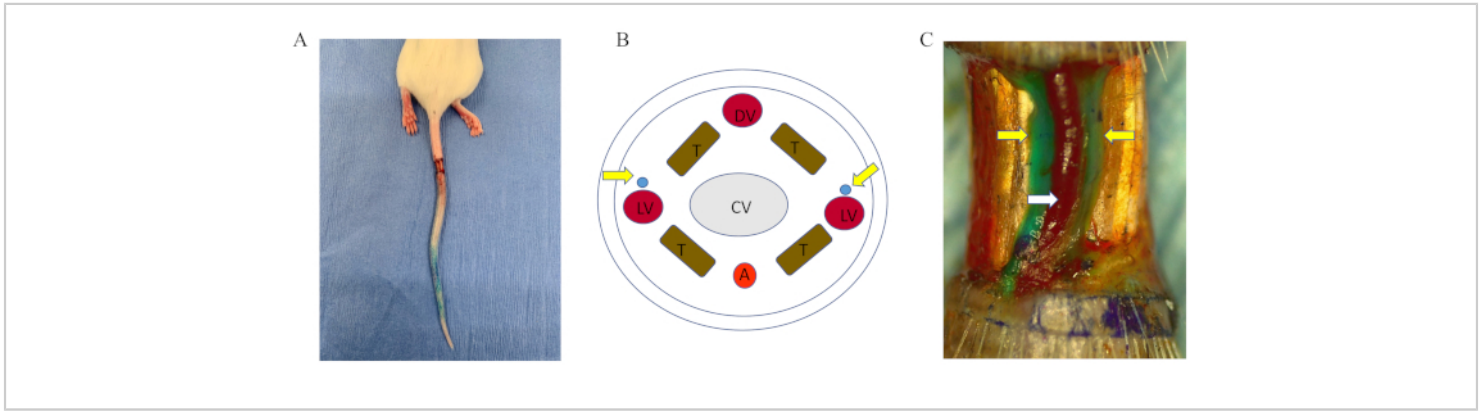

Figure 1: Mouse tail model for sustained lymphedema. (**A**) A 3 mm wide full-thickness skin excision is performed on a murine tail 20 mm from the base under the surgical micrscope. Care is taken to preserve the vasculature. (**B**) A schematic of the cross-section of the mouse tail. DV=dorsal vein, LV=lateral veins, A=ventral caudal artery, CV=caudal vertebra, T=tendon and muscle, yellow arrows shows the lymphatics. (**C**) Following administration of isosulfan blue into the tail tip to localize the lymphatics, the lymphatics (yellow arrow) exhibit blue color. The lymphatics are disrupted while preserving the adjacent lateral veins (white arrow). Please click here to view a larger version of this figure.

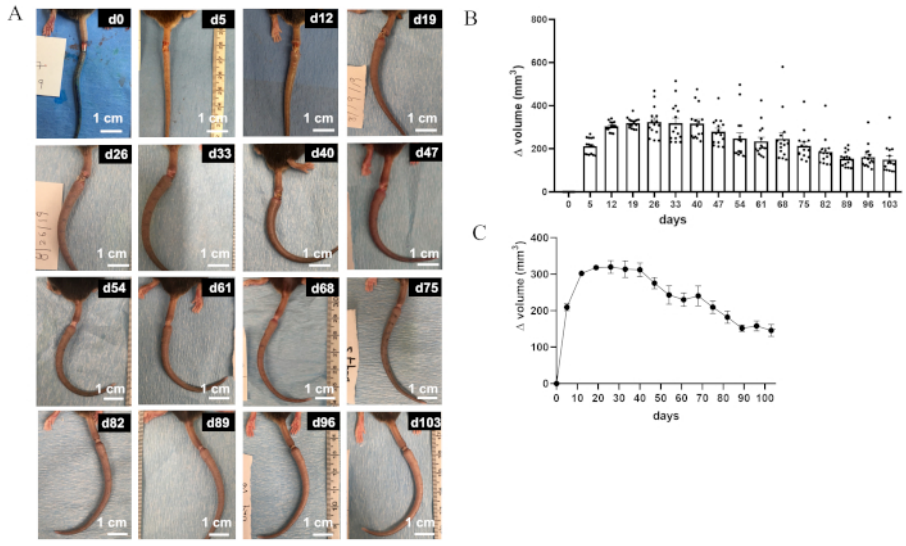

Figure 2: Progressive swelling of the mouse tail lymphedema model. (**A**) Following full-thickness skin excision and lymphatic transection, the mouse tail exhibits progressive swelling that is sustained over 15 weeks. The bracket denotes 20 mm from the base of the tail to the start of the surgical full thickness skin excision. (**B-C**) Quantification of the change in tail volume over 15 weeks represented as (**B**) bar graphs, each dot representing an animal, n=15, or as (**C**) line graph. Data represented as ± SEM. Please click here to view a larger version of this figure.

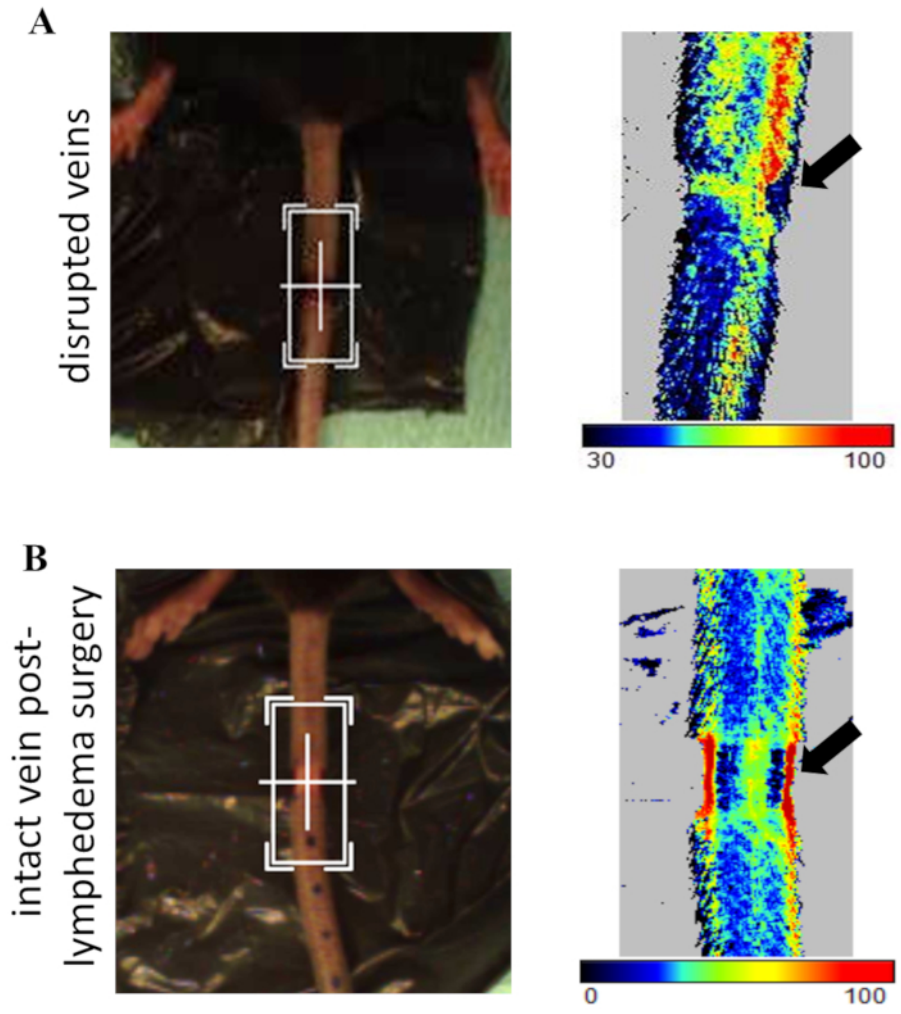

Figure 3: High resolution laser speckle contrast imaging to confirm mouse tail perfusion in the lymphedema mouse tail model. Laser speckle is used to assess mouse tail vasculature postoperatively to validate swelling of lymphatic etiology and minimize tail necrosis. (**A**) A mouse tail with injured lateral veins (black arrow) detected by laser speckle. (**B**) Intact lateral tail vein (black arrow) post-lymphedema surgery detected by laser speckle. (n=5) resolution 0.02 mm; Color coded bar indicates perfusion (blue: low, red: high) as measured in arbitrary relative units. Please click here to view a larger version of this figure.

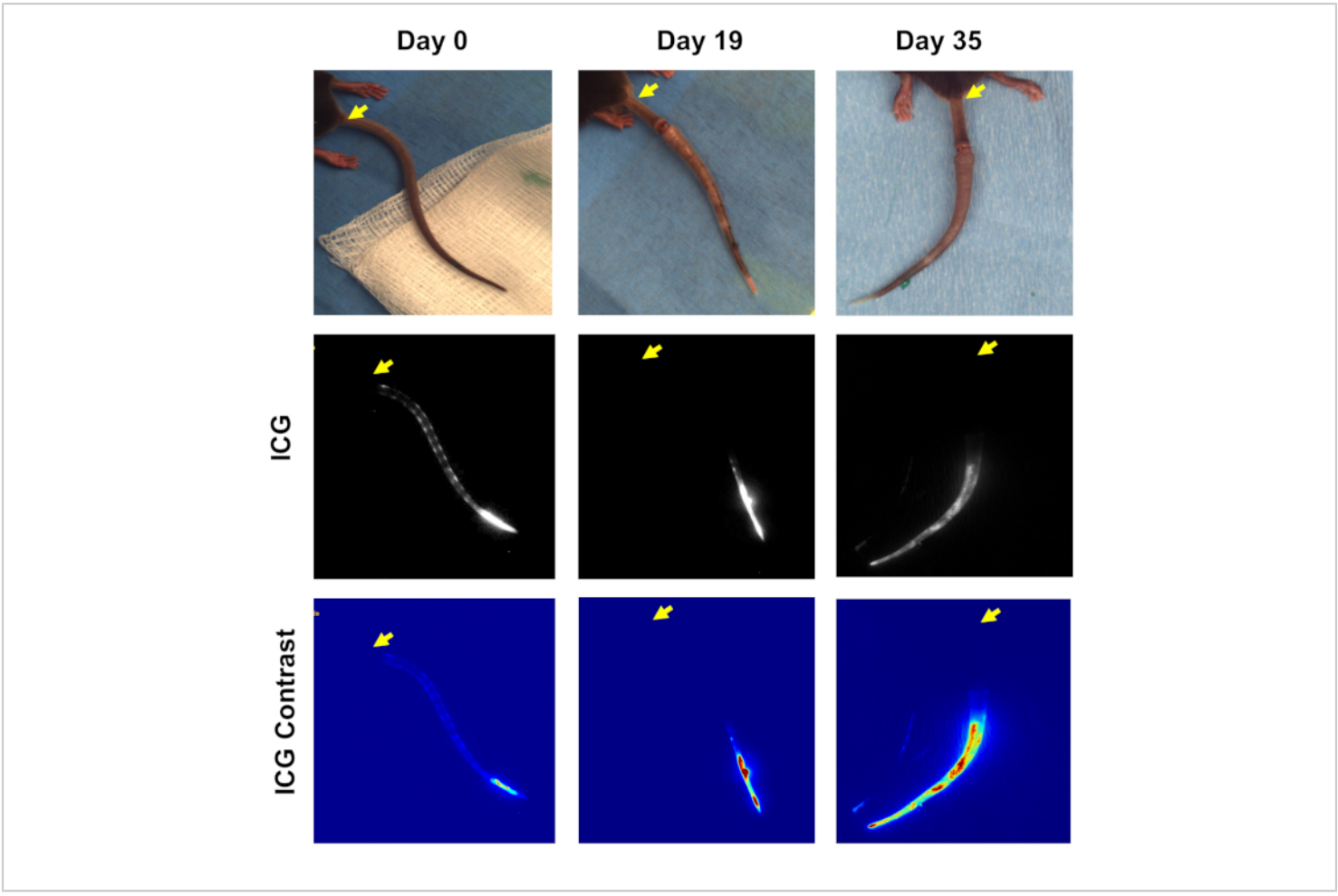

Figure 4: Assessment of lymphatic function using near infrared laser lymphangioraphy in the mouse tail model. Indocyanine green (ICG) injected into the tip of the mouse tail localizes to the lymphatics. Preoperatively, the lymphatics are intact along the mouse tail. Postoperatively, there is no ICG transit beyond the surgical site, confirming that swelling is caused by lymphatic dysfunction. Yellow arrow indicates the base of the tail. Please click here to view a larger version of this figure.

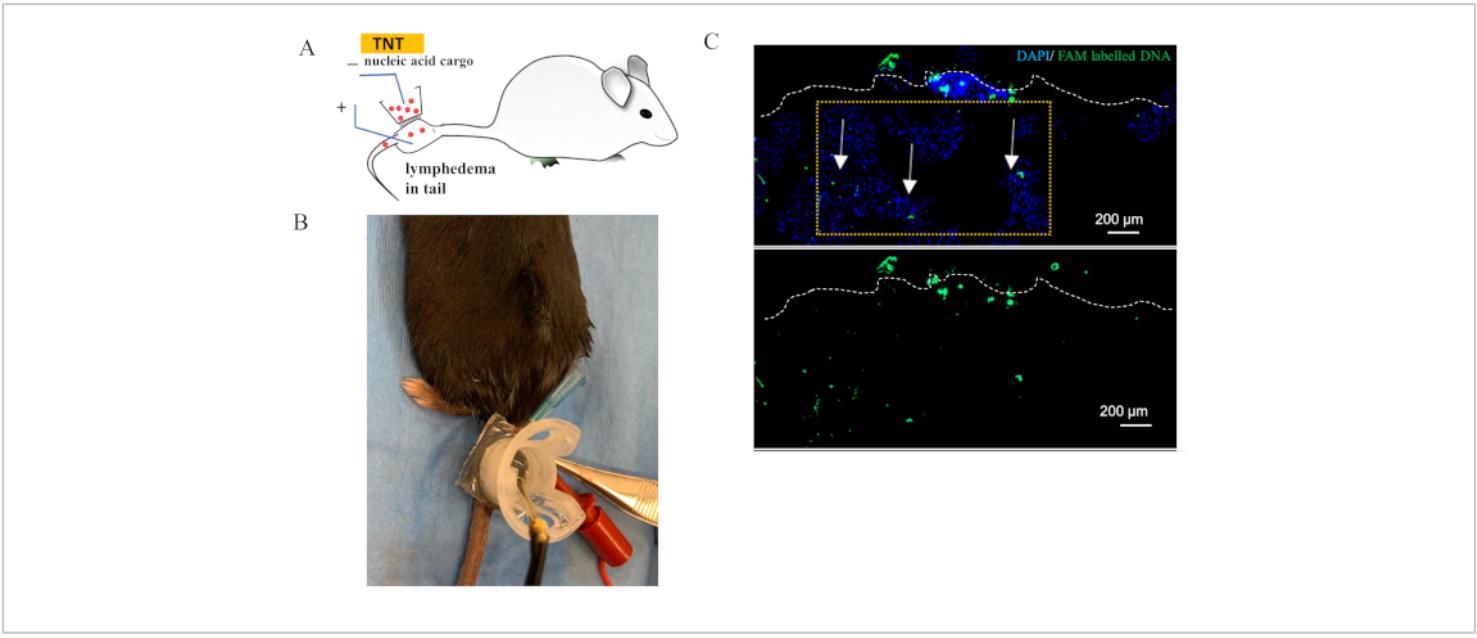

Figure 5: Focal delivery of genetic cargo using tissue nanotransfection technology (TNT). (**A**) Illustration of TNT delivery. (**B**) Plasmids are loaded into the $TNT_{2.0}$ reservoir. The positive and negative electrical probes are attached and a brief, square wave pulse electric stimulation is delivered (10 x 10 ms pulses, 250 V, 10 mA), facilitating focal, non-viral, transcutaneous transfection. (**C**) Efficiency of genetic cargo delivery using $TNT_{2.0}$ as observed through fluorescein amidite (FAM) labeled DNA delivery to the murine tail. Mouse tails were sectioned two days after TNT treatment and assessed through fluorescence microscopy. White dotted lines indicate the epithelium of the skin of murine tail. White arrows indicate the FAM labelled DNA. Please click here to view a larger version of this figure.

Discussion

Lymphedema is categorized as a primary (congenital) or secondary (iatrogenic lymphatic) injury[38,39]. Secondary lymphedema comprises 99% of cases[39]. Secondary lymphedema is most commonly caused by infection (filariasis) or post-oncological treatment with lymphadenectomy or radiation[4,39]. A translational animal model is challenging for secondary lymphedema, as 70% of animals treated with lymphadectomy and radiation do not acquire lymphedema[2,16]. In addition, phenotypical lymphedema exhibits a delayed onset (one year) post-lymphatic injury. The mouse tail model of lymphedema overcomes these obstacles, as all mice undergoing focal tail lymphatic excision exhibit lymphedema within days following the procedure[21,23]. Full thickness focal subcutaneous excision is performed under visualization with the surgical microscope allowing definitive identification of the tissue plane between the tail veins and the subcutaneous tissues and facilitating vessel preservation. We have previously ligated the lymphatic channel with nylon suture, but as persistent lymphedema can be induced with transection of the lymphatic channel only, ligation must be deemed unnecessary. The two lateral lymphatic channels in the mouse tail are in close proximity with the lateral tail veins. Histologically, the swollen tail displays inflammation, intersitial

fluid retention, adipose deposition, and fibrosis, similar to clinical lymphedema[24,27,28,40].

One pitfall of this model is the risk of injury to the lateral veins and vasculature. Performing the procedure on full thickness skin excision using loupe magnification can lead to inadvertent venous bleeding during dissection. Careful excision under high stereoscopic magnification facilitates greater precision for staying within the a vascular plane between the vessel adventitia and subdermal layer. Another difficulty is that tail necrosis occurs with a frequency as high as 30%[30], as vessel injury greatly increases tail necrosis risk. The model marginalizes tail necrosis with (1) the use of a surgical microscope for meticulous dissection and (2) the confirmation of vessel patency by laser speckle imaging[41]. If vascular injury is identified, the animal should be removed from the study. Other investigators have used intracardiac microsphere injection to assess arterial perfusion[22]. Laser speckle imaging allows quantification of the blood flow kinetics of veins in addition to arteries[41]. This minimally invasive technique can provide precise microperfusion data.[41]

The tail volume is used as a phenotypic outcome variable of the model. Assessing lymphatic function of the tail in the model also is used to assess the experimental effect. We use near infrared laser lymphangiography to evaluate lymphatic function in the mouse tail. This directly visualizes real time lymphatic flow in the live animal. ICG laser lymphangiography is also commonly used clinically during lymphatic microsurgical threapeutic procedures such as lymphovenous anastomosis so it translates well[10]. Clinically, this facilitates introperative lymphatic mapping and the identification of target lymphatic vessels to connect them into veins in lymphovenous anatomosis to treat lymphedema[7,10].

One pitfall of using ICG laser lymphangiography is the ease with which the mouse tail and other materials can become coated with ICG, resulting in non-speciic fluoresence and hindering proper visualization of the lymphatics. Therefore, we change gloves immediately both after ICG handling and administration to minimize this risk.

TNT was developed initially for in vivo tissue reprogramming[33]. It is used as a gene transfer platform, more broadly including the rescue of diabetic peripheral neuropathy and the repair of crushed nerves[34,36] and utilizes three essential components: (1) a silicone nanochip for nanoneedle based gene transfer; (2) a nucleic acid cargo (plasmids with ORF or siRNAs); and (3) a standard power supply. TNT facilitates direct, transcutaneous, non-viral gene delivery with a rapid focused electric field. It has been used to decrease limb ischemia by increasing neovascularization in a mouse model[33]. More recently, $TNT_{2.0}$ has been used to label wound-site exosomes[35]. Using TNT in the mouse tail lymphedema model offers an exciting future for the delivery of gene-based therapies.

A translational limitation of the mouse tail lymphedema model has been the spontaneous resolution of lymphedema[21,22], as tail swelling resolves after 20-30 days in some experimental models[21]. In the model, tail swelling volume, as measured by the commonly used truncated cone equation[37], has been sustained for 15 weeks without exhibiting resolution. Perhaps the technique enhancements have maximized persistence of lymphedema. The technique modifications include complete dissection under microcopic magnification, laser speckle evaluation of tail vasculature to ensure rigor for lymphatic origin of lymphedema, functional assessment with ICG laser lymphangiography, and $TNT_{2.0}$ for therapeutic gene delivery. The modified mouse tail model of lymphedema

is a reproducible and clinically translatable animal model of lymphedema.

Disclosures

The authors have no competing conflicts of interest.

Acknowledgments

This work was supported by grant funding provided by the American Association of Plastic Surgeons Academic Scholarship and the Department of Defense W81XWH2110135 to AHH. Aesthetic Surgery Education and Research Foundation grant to MS. NIH U01DK119099, R01NS042617 and R01DK125835 to CKS.

References

1. Kataru, R. P. et al. Fibrosis and secondary lymphedema: chicken or egg? *Translation Research.* **209**, 68-76 (2019).
2. Brayton, K. M. et al. Lymphedema prevalence and treatment benefits in cancer: impact of a therapeutic intervention on health outcomes and costs. *PLoS One.* **9** (12), e114597 (2014).
3. Mendoza, N., Li, A., Gill, A., Tyring, S. Filariasis: diagnosis and treatment. *Dermatology and Therapy.* **22** (6), 475-490 (2009).
4. Rockson, S. G., Rivera, K. K. Estimating the population burden of lymphedema. *Annals of the New York Academy of Sciences.* **1131**, 147-154 (2008).
5. Soran, A. et al. Breast cancer-related lymphedema--what are the significant predictors and how they affect the severity of lymphedema? *Breast Journal.* **12** (6), 536-543 (2006).
6. Hayes, S. C. et al. Upper-body morbidity after breast cancer: incidence and evidence for evaluation, prevention, and management within a prospective surveillance model of care. *Cancer.* **118** (8 Suppl), 2237-2249 (2012).
7. Carl, H. M. et al. Systematic Review of the Surgical Treatment of Extremity Lymphedema. *Journal of Reconstructive Microsurgery.* **33** (6), 412-425 (2017).
8. Garza, R., 3rd, Skoracki, R., Hock, K., Povoski, S. P. A comprehensive overview on the surgical management of secondary lymphedema of the upper and lower extremities related to prior oncologic therapies. *BMC Cancer.* **17** (1), 468 (2017).
9. Hassanein, A. H. et al. Deep Inferior Epigastric Artery Vascularized Lymph Node Transfer: A Simple and Safe Option for Lymphedema. *Journal of Plastic, Reconstructive, Aesthetic Surgery.* **73** (10), 1897-1916 (2020).
10. Hassanein, A. H., Sacks, J. M., Cooney, D. S. Optimizing perioperative lymphatic-venous anastomosis localization using transcutaneous vein illumination, isosulfan blue, and indocyanine green lymphangiography. *Microsurgery.* **37** (8), 956-957 (2017).
11. Chang, D. W., Masia, J., Garza, R., 3rd, Skoracki, R., Neligan, P. C. Lymphedema: Surgical and Medical Therapy. *Plastic and Reconstructive Surgery.* **138** (3 Suppl), 209S-218S (2016).
12. Gould, D. J., Mehrara, B. J., Neligan, P., Cheng, M. H., Patel, K. M. Lymph node transplantation for the treatment of lymphedema. *Journal of Surgical Oncology.* **118** (5), 736-742 (2018).

13. Cook, J. A. et al. Immediate Lymphatic Reconstruction after Axillary Lymphadenectomy: A Single-Institution Early Experience. *Annals of Surgical Oncology.* (2020).
14. Cook, J. A., Hassanein, A. H. ASO Author Reflections: Immediate Lymphatic Reconstruction: A Proactive Approach to Breast Cancer-Related Lymphedema. *Annals of Surgical Oncology.* (2020).
15. Johansson, K., Branje, E. Arm lymphoedema in a cohort of breast cancer survivors 10 years after diagnosis. *Acta Oncologica.* **49** (2), 166-173 (2010).
16. Johnson, A. R. et al. Lymphedema Incidence After Axillary Lymph Node Dissection: Quantifying the Impact of Radiation and the Lymphatic Microsurgical Preventive Healing Approach. *Annals of Plastic Surgery.* **82** (4S Suppl 3), S234-S241 (2019).
17. Gartner, R., Mejdahl, M. K., Andersen, K. G., Ewertz, M., Kroman, N. Development in self-reported arm-lymphedema in Danish women treated for early-stage breast cancer in 2005 and 2006--a nationwide follow-up study. *Breast.* **23** (4), 445-452 (2014).
18. Shin, W. S., Rockson, S. G. Animal models for the molecular and mechanistic study of lymphatic biology and disease. *Annals of the New York Academy of Sciences.* **1131**, 50-74 (2008).
19. Tobbia, D. et al. Lymphedema development and lymphatic function following lymph node excision in sheep. *Journal of Vascular Research.* **46** (5), 426-434 (2009).
20. Olszewski, W., Machowski, Z., Sokolowski, J., Nielubowicz, J. Experimental lymphedema in dogs. *Journal of Cardiovascular Surgery.* **9** (2), 178-183 (1968).
21. Rutkowski, J. M., Moya, M., Johannes, J., Goldman, J., Swartz, M. A. Secondary lymphedema in the mouse tail: Lymphatic hyperplasia, VEGF-C upregulation, and the protective role of MMP-9. *Microvascular Research.* **72** (3), 161-171 (2006).
22. Tabibiazar, R. et al. Inflammatory manifestations of experimental lymphatic insufficiency. *PLoS Medicine.* **3** (7), e254 (2006).
23. Slavin, S. A., Van den Abbeele, A. D., Losken, A., Swartz, M. A., Jain, R. K. Return of lymphatic function after flap transfer for acute lymphedema. *Annals of Surgery.* **229** (3), 421-427 (1999).
24. Zampell, J. C. et al. Toll-like receptor deficiency worsens inflammation and lymphedema after lymphatic injury. *American Journal of Physiology-Cell Physiology.* **302** (4), C709-719 (2012).
25. Gardenier, J. C. et al. Diphtheria toxin-mediated ablation of lymphatic endothelial cells results in progressive lymphedema. *JCI Insight.* **1** (15), e84095 (2016).
26. Weiler, M. J., Cribb, M. T., Nepiyushchikh, Z., Nelson, T. S., Dixon, J. B. A novel mouse tail lymphedema model for observing lymphatic pump failure during lymphedema development. *Scientific Reports.* **9** (1), 10405 (2019).
27. Avraham, T. et al. Th2 differentiation is necessary for soft tissue fibrosis and lymphatic dysfunction resulting from lymphedema. *FASEB J.* **27** (3), 1114-1126 (2013).
28. Zampell, J. C. et al. CD4(+) cells regulate fibrosis and lymphangiogenesis in response to lymphatic fluid stasis. *PLoS One.* **7** (11), e49940 (2012).
29. Arruda, G., Ariga, S., de Lima, T. M., Souza, H. P., Andrade, M. A modified mouse-tail lymphedema model. *Lymphology.* **53** (1), 29-37 (2020).

30. Jun, H. et al. Modified Mouse Models of Chronic Secondary Lymphedema: Tail and Hind Limb Models. *Annals of Vascular Surgery.* **43**, 288-295 (2017).

31. Karkkainen, M. J. et al. A model for gene therapy of human hereditary lymphedema. *Proceedings of the National Academy of Sciences of the United States of America.* **98** (22), 12677-12682 (2001).

32. Yoon, Y. S. et al. VEGF-C gene therapy augments postnatal lymphangiogenesis and ameliorates secondary lymphedema. *Journal of Clinical Investigation.* **111** (5), 717-725 (2003).

33. Gallego-Perez, D. et al. Topical tissue nano-transfection mediates non-viral stroma reprogramming and rescue. *Nature Nanotechnology.* **12** (10), 974-979 (2017).

34. Moore, J. T. et al. Nanochannel-Based Poration Drives Benign and Effective Nonviral Gene Delivery to Peripheral Nerve Tissue. *Advanced Biosystems.* e2000157 (2020).

35. Zhou, X. et al. Exosome-Mediated Crosstalk between Keratinocytes and Macrophages in Cutaneous Wound Healing. *ACS Nano.* **14** (10), 12732-12748 (2020).

36. Roy, S. et al. Neurogenic tissue nanotransfection in the management of cutaneous diabetic polyneuropathy. *Nanomedicine.* **28**, 102220 (2020).

37. Sitzia, J. Volume measurement in lymphoedema treatment: examination of formulae. *European Journal of Cancer Care.* **4** (1), 11-16 (1995).

38. Smeltzer, D. M., Stickler, G. B., Schirger, A. Primary lymphedema in children and adolescents: a follow-up study and review. *Pediatrics.* **76** (2), 206-218 (1985).

39. Maclellan, R. A., Greene, A. K. Lymphedema. *Seminars in Pediatric Surgery.* **23** (4), 191-197 (2014).

40. Clavin, N. W. et al. TGF-beta1 is a negative regulator of lymphatic regeneration during wound repair. *American Journal of Physiology: Heart and Circulatory Physiology.* **295** (5), H2113-2127 (2008).

41. Gnyawali, S. C. et al. Retooling Laser Speckle Contrast Analysis Algorithm to Enhance Non-Invasive High Resolution Laser Speckle Functional Imaging of Cutaneous Microcirculation. *Scientific Reports.* **7**, 41048 (2017).